



HAL
open science

Synergistic convergence of microbiota-specific systemic IgG and secretory IgA

Karim Dorgham, Hela El Kafsi, Sébastien Andre, Eric Oksenhendler, Jehane Fadlallah, Delphine Sterlin, Claire Fieschi, Christophe Parizot, Gaëlle Autaa, Pascale Ghillani-Dalbin, et al.

► **To cite this version:**

Karim Dorgham, Hela El Kafsi, Sébastien Andre, Eric Oksenhendler, Jehane Fadlallah, et al.. Synergistic convergence of microbiota-specific systemic IgG and secretory IgA. *Journal of Allergy and Clinical Immunology*, 2019, 143 (4), pp.1575-1585.e4. 10.1016/j.jaci.2018.09.036 . hal-02171187

HAL Id: hal-02171187

<https://hal.sorbonne-universite.fr/hal-02171187>

Submitted on 29 Aug 2019

HAL is a multi-disciplinary open access archive for the deposit and dissemination of scientific research documents, whether they are published or not. The documents may come from teaching and research institutions in France or abroad, or from public or private research centers.

L'archive ouverte pluridisciplinaire **HAL**, est destinée au dépôt et à la diffusion de documents scientifiques de niveau recherche, publiés ou non, émanant des établissements d'enseignement et de recherche français ou étrangers, des laboratoires publics ou privés.

1 Synergistic convergence of microbiota-specific systemic IgG and secretory IgA

2 Jehane Fadlallah^{1,3†}, Delphine Sterlin^{1†}, Claire Fieschi³, Christophe Parizot¹, Karim 3 Dorgham¹,
Hela El Kafsi¹, Gaëlle Autaa¹, Pascale Ghillani-Dalbin¹, Catherine Juste², Patricia Lepage², 4
Marion Malphettes³, Lionel Galicier³, David Boutboul³, Karine Clément^{4,5,6,7}, Sébastien 5
André^{4,5,6}, Florian Marquet^{4,5,6}, Christophe Tresallet⁸, Alexis Mathian¹, Makoto Miyara¹, Eric 6
Oksenhendler³, Zahir Amoura¹, Hans Yssel¹, Martin Larsen^{1*}, Guy Gorochov^{1*}

7

8 Affiliations:

9

10 ¹Sorbonne Université, INSERM, Centre d'Immunologie et des Maladies Infectieuses (CIMI-
11 Paris), AP-HP Hôpital Pitié-Salpêtrière, F-75013 Paris, France

12 ²UMR1319 Micalis, INRA, Jouy-en-Josas, France.

13 ³Université Paris Diderot Paris 7, Department of Clinical Immunology, Hôpital Saint-Louis,
14 Assistance Publique Hôpitaux de Paris (APHP), EA3518, 75010, Paris, France

15 ⁴INSERM, UMR_S 1166, NutriOmics Team, F-75013, Paris, France;

16 ⁵Sorbonne Universités, UPMC University Paris 06, UMR_S 1166, F-75005, Paris, France;

17 ⁶Institute of Cardiometabolism and Nutrition, ICAN, Pitié-Salpêtrière Hospital, Assistance
18 Publique Hôpitaux de Paris, F-75013, Paris, France;

19 ⁷Assistance Publique Hôpitaux de Paris, Pitié-Salpêtrière Hospital, Nutrition, Endocrinology
20 Departments, F-75013, Paris, France

21 ⁸Assistance Publique Hôpitaux de Paris, Pitié-Salpêtrière Hospital, Department of surgery, F-
22 75013, Paris, France

23

24

25 †These authors contributed equally to this work

26 *To whom correspondence should be addressed: guy.gorochov@upmc.fr or
27 martin.larsen@upmc.fr.

28

29 **Conflict of interests:** The authors declare no competing interests.

30 **Funding:** The study was financed by Institut national de la santé et de la recherche médicale
31 (Inserm) and Agence Nationale de la Recherche (MetAntibody ANR)

32

33 **Abstract (<250 words)**

34

35 **Background:** Besides intestinal barrier function, the host tolerates gut commensals through
36 both innate and adaptive immune mechanisms. It is now clear that gut commensals induce
37 local immunoglobulin A (IgA) responses, but it remains unclear whether anti-microbiota
38 responses remain confined to the gut.

39 **Objective:** The aim of this study was to investigate systemic and intestinal responses against
40 the whole microbiota under homeostatic conditions, and in the absence of IgA.

41 **Methods:** We analyzed blood and feces from healthy donors, patients with selective IgA
42 deficiency (SIgAd) and common variable immunodeficiency (CVID). Immunoglobulin-
43 coated bacterial repertoires were analyzed by combined bacterial fluorescence-activated cell
44 sorting and 16S rRNA sequencing, and bacterial lysates were probed by western blot analysis
45 with healthy donors serums.

46 **Results:** Although absent from the healthy gut, serum anti-microbiota IgG are present in
47 healthy individuals, and increased in SIgAd patients. IgG converge with non-overlapping
48 secretory IgA repertoires to target the same bacteria. Each individual targets a diverse,
49 microbiota repertoire whose proportion inversely correlates with systemic inflammation.
50 Finally, Intravenous Immunoglobulin preparations (IVIG) target much less efficiently CVID
51 gut microbiota than healthy microbiota.

52 **Conclusion:** Secretory IgA is pivotal for induction of tolerance to gut microbiota. SIgAd-
53 associated inflammation is inversely correlated with systemic anti-commensal IgG responses,
54 which may thus serve as a second line of defense. We speculate that SIgAd patients could
55 benefit from oral IgA supplementation. Our data also suggest that IVIG preparations might be
56 supplemented with IgG from IgA deficient patients pools in order to offer a better protection
57 against gut bacterial translocations in CVID.

58

59

60 **Key Messages:**

61

62 - Systemic IgG and secretory IgA bind a common spectrum of commensals.

63 - Increased proportions of IgG+ microbiota and inflammatory markers in SIgAd.

64 - IVIG poorly target CVID and SIgAd gut microbiota.

65 **Capsule summary:**

66 Serum anti-microbiota IgG are present in healthy individuals, and increased in SIgAd. IVIG

67 only bind a small fraction of SIgAd gut microbiota. Oral IgA and IgA/IgG supplementation

68 should be considered in SIgAd and CVID, respectively.

69 **Key words (<10):** gut microbiota, anti-commensal IgG, secretory IgA, IgA deficiency,

70 CVID, IVIG.

71

72 **Abbreviations:**

73 Ig: Immunoglobulin

74 SIgAd : Selective IgA deficiency

75 CVID: Common Variable Immunodeficiency

76 IVIG: Intravenous Immunoglobulin

77

78 **Acknowledgments:** The authors wish to thank Emma Slack for advice, Jean-Michel Batto for

79 discussions, Joel Doré, Fabienne Beguet-Crespel and Emma Slack for providing bacterial

80 strains.

81 **Funding:** The study was financed by: Institut national de la santé et de la recherche médicale

82 (Inserm), Agence Nationale de la Recherche (MetAntibody, ANR-14-CE14-0013), Fondation

83 pour l'Aide a la Recherche sur la Sclérose En Plaques (ARSEP).

84

85

86

87 Introduction

88

89 Gut commensal bacteria contribute to several beneficial properties to the host. This complex
90 community provides metabolic functions, prevents pathogen colonization and enhances
91 immune development. A symbiotic relationship is maintained using host innate and adaptive
92 immune responses such as antimicrobial compounds and mucus secretion, as well as IgA
93 production^{1,2}. However, the gastrointestinal tract remains an important reservoir for potential
94 bloodstream infections that involve *Enterobacteriaceae*, *Enterococcus* species or other Gram-
95 negative bacilli^{3,4}. The physical gut barrier, but also innate and adaptive immune
96 mechanisms, control host-microbiota mutualism, reducing the risk of bacterial translocation
97 and systemic immune activation. Murine models of innate immune deficiency indeed develop
98 high seric IgG levels against gut microbiota². Significant titers of IgG targeting *E. coli* were
99 also reported either in patients with inflammatory bowel diseases or in mice lacking secretory
100 IgA^{5,6}. Nevertheless, based on recent murine studies, the notion has emerged that induction
101 of systemic IgG responses against gut symbiotic bacteria is not necessarily a consequence of
102 mucosal immune dysfunction or epithelial barrier leakiness. Healthy mice actively generate
103 systemic IgG against a wide range of commensal bacteria under homeostatic conditions,
104 which are passively transferred to the neonates through the maternal milk⁷. Serum IgG that
105 specifically recognize symbiotic Gram-negative bacteria confer protection against systemic
106 infections by these same bacteria. Because such IgG target a conserved antigen in commensal
107 and pathogens, they also enhance elimination of pathogens such as *Salmonella*⁸.

108 IgG-expressing B cells are present in human gut lamina propria during steady state
109 conditions, and represent 3-4% of the total gut B cells. About two-third of IgG+ lamina
110 propria antibodies react with common intestinal microbes⁹. Inflammatory bowel disease is
111 associated with a marked increase in gut IgG⁺ B cells that might contribute to the observed
112 elevated serum anti-*E. coli* IgG levels in these patients⁹. However, to which extent gut IgG⁺

113 B cells contribute to the serum IgG repertoire, remains elusive. Focusing on anti-
114 transglutaminase 2 antibodies, it has been shown a low degree of clonal relationship between
115 serum and intestinal IgG ¹⁰. Altogether, it remains unknown whether secretory and serum
116 anti-bacteria antibodies have identical targets or whether digestive and systemic antibody
117 repertoires are shaped by distinct microbial consortia.

118

119 In this study, we report that human serum IgG bind a broad range of commensal bacteria. We
120 also demonstrate for the first time the convergence of intestinal IgA and serum IgG responses
121 toward the same microbial targets, under homeostatic conditions. Private anti-microbiota IgG
122 specificities are induced in IgA-deficient patients, but are not found in IgG pools from healthy
123 donors, partially explaining why substitutive IgG cannot regulate antibody deficiency-
124 associated gut dysbiosis and intestinal translocation. Finally, in both controls and IgA-
125 deficient patients, systemic anti-microbiota IgG responses correlate with reduced
126 inflammation suggesting that systemic IgG responses contribute to the gut microbiota
127 confinement.

128

129

130

131

132

133 **Results**

134

135 **1/ Convergence of intestinal IgA and serum IgG toward the same bacterial cells**

136 To determine the level of humoral systemic response against fecal microbiota, we have
137 elaborated a flow cytometric assay derived from a previously reported technology ¹¹. This
138 protocol allows to probe concomitantly IgA and IgG microbiota coating. We found that
139 approximately 8% of the fecal microbiota is targeted by secretory IgA (median[*min-max*];
140 8[0.8-26.7]%; n=30) in healthy donors, in concordance with previous reports ¹². As shown,
141 the proportion of bacteria *in vivo* bound by secretory IgA in human feces is highly variable
142 between healthy individuals (Figure 1B). IgG-bound bacteria are virtually absent from healthy
143 human feces (median [*min-max*]; 0.03[0-0.16]%; n=30 ; Figure S1 and 1A), in agreement
144 with the lack of IgG transport to the intestinal lumen. In healthy donors, seric IgG bound a
145 median rate of 1.1% of fecal bacteria (median [*min-max*]; 1.1[0.2-3.2]%; Figure 1B).
146 Surprisingly, seric IgG targeted exclusively secretory IgA bound bacteria (Figure 1A).
147 Conversely, all IgA-coated bacteria (IgA⁺ bacteria) were not targeted by seric IgG. Of note,
148 an irrelevant human monoclonal IgG (chimeric anti-human TNF containing a human Fc IgG
149 fraction) exhibits markedly reduced binding to IgA⁺ bacteria, compared to serum IgG (Figure
150 1A, S2), demonstrating that IgG binding to IgA-coated bacteria is mostly Fab-mediated.

151 To confirm that systemic IgG binding is directed against IgA-bound bacteria, we evaluated *in*
152 *vitro* serum IgG binding to cultivable bacterial strains. We selected four bacterial strains that
153 were not preferentially bound by IgA in human feces and four others that were previously
154 defined as classical IgA targets *in vivo* ¹²⁻¹⁴. As shown in Figure 2, IgG from healthy
155 individuals (n = 30) bind much more significantly *Bifidobacterium longum*, *Bifidobacterium*
156 *adolescentis*, *Faecalibacterium prausnitzii* and *Escherichia coli*, known to be particularly
157 enriched in the IgA-coated fraction of healthy individuals, than three different strains of
158 *Bacteroides sp.* and *Parabacteroides distasonis*, known to be particularly enriched in the IgA-

159 uncoated fraction of the fecal microbiota (Figure 2A-B). The majority of anti-commensal IgG
160 antibodies are of the IgG2b and IgG3 isotypes in mice. Using isotype-specific secondary
161 antibodies we detected minimal IgG1 binding, but high seric IgG2 reactivity, to
162 *Bifidobacterium adolescentis*, *Bifidobacterium longum* and *Escherichia coli*, suggesting that
163 IgG2 is involved in commensals targetting in humans (Figure S3).

164 Since anti-commensal IgG might possibly be triggered during mucosal immune responses, we
165 characterized lamina propria B cells and detected the presence of IgG2+ B cells throughout
166 the intestine (Figure S4). Of note, IgG transcripts are more abundant in LP tissue than in
167 PBMCs, as measured by qPCR (Figure S4).

168 These results demonstrate that human IgG recognize a wide range of commensal under
169 homeostatic conditions. Systemic humoral immunity (notably IgG2) converges with mucosal
170 immunity to bind the surface of commensals.

171

172 **2/ Inter-individual variability and non overlapping anti-commensal IgA and IgG** 173 **molecular targets.**

174

175 It was previously suggested that murine IgG would target a restricted number of bacterial
176 proteins and favored highly conserved outer membrane proteins⁸. Reactivity of human serum
177 IgG against bacterial lysates from a Gram-negative strains was evaluated by immunoblotting.

178 We observed that IgG labeled several *E. coli* bands (Figure 2C), suggesting that multiple
179 bacterial products are involved in the induction of systemic antibodies. Interestingly, this
180 analysis reveals a great deal of inter-individual variability, as it is not always the same
181 bacterial products that react with the tested serums. We then compared the overlap between
182 bacterial products labeled by IgG and IgA and found distinct binding profiles (Figure 2C).

183 Finally, in the 5 individuals tested, although some bacterial products (notably a 15 Kd

184 antigen) are frequently targeted in most subjects and without isotype restriction, it clearly
185 appears that IgA and IgG never share exactly the same binding pattern at a molecular level.
186 Taken together, these results demonstrate although IgG converges with IgA to bind the
187 surface of commensals, it appears that IgA and IgG do not systematically target the same
188 bacterial antigens, even at the individual level.

189

190 **3/ Private anti-microbiota IgG specificities are induced in IgA-deficient patients**

191 The existence of seric IgG able to bind IgA-coated bacteria could equally suggest that some
192 gut bacteria (or bacterial antigens) might cross the intestinal barrier: (i) in spite of IgA, or (ii)
193 because of IgA. In order to explore these two putatively opposing roles for IgA, we studied
194 the systemic anti-commensal IgG response in SIgAd. These patients had undetectable seric
195 and digestive IgA levels while seric IgG were in the normal range¹⁵. Anti-microbiota IgG
196 levels were significantly higher in SIgAd compared to controls (median [min-max]%; 3.3[0.2-
197 20.2]% *versus* 1.1%[0.2-3.2]%; Figure 3A). Using irrelevant human IgG, we confirmed that,
198 like in healthy donors, IgG interact with fecal bacteria in a Fab-dependent manner (Figure
199 S2B). These data support an enhanced triggering of systemic IgG immunity against fecal
200 microbiota when lacking secretory IgA, as shown in the murine model of polymeric
201 immunoglobulin receptor deficiency ⁶.

202 Considering this high level of anti-microbiota IgG in SIgAd, and the similarity of SIgAd and
203 healthy microbiota composition¹⁵, we investigated how anti-microbiota IgG repertoires from
204 healthy donors and IgA deficient patients were overlapping. Using polyclonal IgG from
205 pooled serum of healthy donors, we assessed IgG-bound microbiota using either healthy or
206 SIgAd purified microbiota. We showed that pooled polyclonal IgG and autologous healthy
207 sera recognized a similar percentage of fecal bacteria (median [min-max]%; 1[0-3.7] % *vs*
208 1.1[0.2-3.2]%, respectively, figure 3B-C). In contrast, pooled polyclonal IgG bound a smaller

209 bacterial fraction of IgA deficient-microbiota compared to autologous patient serum (median
210 [min-max]%;0.4[0-3.6] % vs 3.3[0.2-20.2] %, figure 3B-C). In order to test whether similar
211 specificities are induced in all or most IgA deficient individuals, we compared their IgG
212 reactivity to autologous or heterologous gut microbiota. In this experiment (Figure 3D), each
213 IgA-deficient microbiota was incubated either with autologous serum (*i.e.*: autologous
214 condition), or with serum from an unrelated IgA deficient individual (*i.e.*: heterologous
215 condition). As shown in Figure 3D, no significant difference was seen between autologous or
216 heterologous conditions (median autologous IgG⁺ microbiota 1.2% *versus* median
217 heterologous IgG⁺ microbiota 1.4%). Of note, heterologous seric IgG also predominantly
218 interact with fecal microbiota in a Fab-dependent manner (Figure S2C).
219 This set of data suggests that peculiar anti-microbiota IgG specificities are induced in IgA-
220 deficient patients, but not in healthy individuals.

221 **4/ IgG specifically recognize a broad spectrum of bacteria**

222 To more deeply decipher anti-commensal IgG specificities in both healthy donors and IgA
223 deficient patients, we next performed a stringent flow-sorting to isolate IgG-bound bacteria
224 and identified their taxonomy by 16S rRNA sequencing (Figure 4A). We observed extensive
225 inter-individual variability at genus level irrespective of immunological status (healthy donors
226 vs IgA deficient patients). Microbial diversity calculated by Shannon index varied between
227 donors, but on average bacterial diversity of IgG⁺ and IgG⁻ bacteria was not significantly
228 different (Figure 4B). We postulated that IgG might preferentially interact with dominant
229 taxa, and therefore compared relative abundance of IgG-bound and IgG-unbound genera.
230 Both fractions exhibited equal distributions of rare and abundant genera (Figure 4C), thus IgG
231 target commensals irrespectively of their frequency. Interestingly, we found that individual
232 IgG⁺ and IgG⁻ fecal bacterial profiles were remarkably different, supporting a strong IgG bias
233 against peculiar taxa that cannot be explained by an expansion of the latter. Besides, anti-

234 commensals IgG were not restricted to pathobionts, but also targeted symbiotic genera such as
235 *Faecalibacterium*, whose the most common species (*i.e.*: *F.prausnitzii*) has been assigned
236 anti-inflammatory properties in both healthy donors and IgA deficient patients (Figure 4D-E)
237 ¹⁶. From this part we conclude that anti-commensal IgG recognize a diverse array of both
238 pathobionts and commensal bacteria. Importantly, each individual harbored a private IgG
239 antimicrobial signature.

240

241 **5/ High anti-microbiota IgG levels correlate with reduced systemic inflammation**

242 Microbiota-specific serum IgG responses contribute to symbiotic bacteria clearance in
243 periphery and maintain mutualism in mice ². We thus hypothesized that anti-commensals IgG
244 might influence the balance of systemic inflammatory versus regulatory responses in humans.
245 Hence, we measured plasma levels of sCD14 (a marker of monocyte activation, ¹⁷) and
246 observed that seric IgG-coated bacteria inversely correlated with soluble CD14 ($r=-0.42$,
247 $p<0.005$; Figure 5A) in both healthy donors and SIgAd patients. These results are in line with
248 the finding that IgG replacement therapy reduced endotoxemia ¹⁸. To further explore the
249 potential link between anti-microbiota IgG and systemic inflammation, we explored CVID
250 patients (characterized by both IgG and IgA defects). These patients benefit from IVIG
251 treatment. Yet, we show that IVIG do not efficiently bind CVID microbiota. As shown in
252 Figure 5B, IVIG bound a reduced fraction of CVID microbiota compared to control
253 microbiota (median [min-max]%; 0.37[0.00-1.14]% vs 1.06[0.00-3.7]%). We then determined
254 plasma levels of sCD14 and IL-6 (an inflammatory cytokine reflecting T-cell activation) and
255 evaluated the expression of PD-1 (a T-cell co-inhibitory molecule induced after activation) on
256 CD4+ T cells. IL-6 as well as sCD14 levels were consistently higher in CVID patients than in
257 healthy donors (IL-6, median [min-max]%, 1.8(0.7-60.1) pg/ml versus 0.6(0.33-2.4) pg/ml;
258 sCD14, median [min-max]%; 2063 (590-5493) pg/ml versus median 2696(1147-4283) pg/ml;

259 Figure 5C-D). Moreover, CD45RA-PD1+CD4+ T cells tended to increase in CVID patients,
260 as compared with healthy donors (median [min-max]%; 20.3(4.26-59.6)% versus 10(2.09-
261 41.9)%, Figure 5E).

262 Altogether, in both controls and IgA-deficient patients, systemic anti-microbiota IgG
263 responses correlate with reduced inflammation.

264

265

266 **Discussion**

267 Anti-commensal IgG have been described in patients with inflammatory diseases^{5,19,20}. Here,
268 we characterize for the first time a broad anti-commensal IgG response under homeostatic
269 conditions in humans. Previous work demonstrated that symbiotic Gram-negative bacteria
270 disseminate spontaneously and drive systemic IgG responses⁸. We show here that a diverse
271 array of commensal bacteria, including Gram-positive and Gram-negative species, can induce
272 systemic IgG. We show that a pathobiont like *E. coli* induce less systemic IgG responses than
273 a presumably beneficial symbiont like *B. adolescentis* (Fig. 2B). Therefore the systemic IgG
274 response in healthy humans does not appear preferentially driven by pathobionts, but also by
275 commensals. In mice it has been shown that commensal microbes induce serum IgA
276 responses that protect against sepsis²¹, illustrating the consequence of systemic anti-microbial
277 IgA binding to both pathogenic strains and commensals. We postulate that systemic anti-
278 microbiota IgG, also mainly induced by commensals, could have the same protective role.
279 Strikingly, systemic IgG and secretory IgA converge towards the same autologous microbiota
280 subset. Yet, it seems unlikely that secretory IgA enhances systemic IgG responses, since IgA
281 deficiency is associated with high proportions of IgG+ microbiota, as detected using bacterial
282 flow cytometry on SIgAd microbiota labeled with autologous serum. In addition, induction of
283 anti-commensal IgG has been shown to be microbiota-dependent, but IgA-independent in
284 mice^{2,6}. Systemic IgG could reflect asymptomatic gut microbiota translocation episodes in
285 healthy individuals. Repeated bacterial translocations might occur more frequently in the
286 absence of secretory IgA, accounting for elevated anti-microbiota IgG levels in these patients.
287 IgA do not activate complement via the classical pathway²². Interestingly, the anti-
288 *Bifidobacterium adolescentis* IgG response is primarily restricted to the IgG2 isotype (Figure
289 S3), which less efficiently triggers the classical route of complement than IgG1 and IgG3²³.
290 Furthermore, IgG2 poorly interact with type I Fc γ Rs, while IgG1 and IgG3 demonstrate

291 affinity for most FcγRs²⁴. These distinct binding patterns have functional consequences. IgG1
292 antibodies mediate phagocytosis and induce potent pro-inflammatory pathways while IgG2
293 are rather involved in dendritic cell or B cell activation^{25,26}. Besides its specific Fc domain
294 interaction, IgG2 is usually, but not exclusively, associated with anti-carbohydrate responses
295²⁷. IgA was also recently shown to bind multiple microbial glycans²⁸. Thus, IgA and IgG2
296 could be viewed as playing similar roles, but in different compartments. Much effort has been
297 recently expended to develop bacterial glycan or protein microarray. Glycomics could
298 represent a new option in order to better decipher anti-microbiota antibody targets^{27,29}.

299 Importantly, we show that IgA and IgG do not systematically target the same bacterial
300 antigens at an individual level (Figure 2C). Therefore IgG and IgA epitopes are not strictly
301 overlapping. This result could further illustrate antibacterial IgA/IgG synergy, and explain the
302 absence of isotype competition allowing the observed IgA/IgG co-staining of bacteria (Figure
303 1).

304 Recent studies suggested that murine secretory IgA are polyreactive and bind a broad but
305 defined subset of microbiota^{30,31}. Similarly, up to 25% of intestinal IgG⁺ plasmablasts could
306 produce polyreactive antibodies⁹. We therefore hypothesized that the cross-reactive potential
307 of anti-commensal IgG may act as a first line of defense against potentially harmful bacteria.
308 In line with this idea, it can be noted that homeostatic anti-commensal IgG confer protection
309 against pathogens such as *Salmonella*⁸. Conversely, IgG directed against *Klebsiella*
310 *pneumoniae*, an opportunistic pathogen, cross-react with commensal microbes³². Clonally
311 related memory B cells expressing cross-specific anti-*K. pneumoniae* antibodies were found
312 in both lamina propria and peripheral blood in humans suggesting that generation of anti-
313 commensal antibodies might be triggered in the mucosal compartment. At the same time,
314 anti-commensal memory B cells might recirculate in periphery³². Altogether, it appears
315 possible that bacteria-specific IgG would arise from the gut, as all bacteria-specific IgG

316 isotypes we characterized in human sera are also present in the gut (Fig. S4), and also because
317 a large proportion of gut IgG+ B cells are expected to be commensal-specific⁹. However, it
318 remains presently unknown whether serum IgG responses mainly originate from the gut
319 and/or are induced the periphery following bacterial translocation.

320 We report that each individual harbors a private set of anti-commensal IgG in both healthy
321 donors and IgA deficient patients. Since our analysis was limited to 3 IgA deficient patients,
322 further study might precisely reveal how SIgAd anti-commensal IgG bind a distinct set of
323 commensals. While IVIG preparations contain an extended set of anti-commensal IgG, we
324 observe that IVIG less efficiently bind CVID microbiota. These observations are consistent
325 with reported alterations of gut microbiota in CVID patients³³. Microbiota perturbations are
326 also associated with selective IgA deficiency. The latter perturbations are less pronounced
327 than in CVID, since the presence of IgM appears to preserve SIgAd microbiota diversity¹⁵.
328 Nevertheless, IgA deficiency condition is also associated in severe cases with bacterial
329 translocation, colitis and dysbiosis. These complications are not accessible to substitutive Ig
330 replacement therapy³⁴. Indeed, IVIG do not appear to contain high-enough concentrations as
331 well as appropriate specificities of anti-commensal IgG. As shown in Figure 3, healthy
332 control serum usually less efficiently binds IgA deficient microbiota than autologous serum.
333 Similarly, IVIG poorly targets CVID gut microbiota (Figure 5B). In addition, local mucosal
334 antibody responses might be important in regulating microbiota composition in a way that
335 cannot be substituted by IVIG. These findings expand our understanding of how IVIG fail to
336 treat gastro-intestinal symptoms in CVID and IgA deficient patients. Dysbiosis and gastro-
337 intestinal complications might not accessible to substitutive Ig replacement therapy, since, as
338 we show, healthy IgG repertoire does not contain adequate “dysbiotic-specific” antibodies.

339

340 It was recently shown in mice that maternally-derived anti-commensal IgG dampen aberrant
341 mucosal immune responses and strengthen epithelial barrier ^{7,35}. The contribution of systemic
342 anti-commensal IgG to the regulation of microbiota/immune homeostasis was not explored in
343 the latter studies. Here, we show that anti-commensal IgG are negatively associated with
344 sCD14, suggesting they might quell inflammation. In support of this, we measured higher
345 levels of sCD14 and IL-6 in plasma of patients lacking both IgA and IgG compared to
346 controls (Figure 5).

347

348 Altogether, these data suggest that systemic IgG and intestinal IgA cooperate in different
349 body compartments to limit systemic pro-inflammatory pathways. While selective IgA
350 deficient patients harbour elevated seric anti commensal IgG levels, CVID patients can not
351 mount an appropriate IgG response. These findings suggest that : in selective IgA deficiency,
352 microbiota confinement is obtained at the price of a strong inflammatory response, and in
353 CVID, confinement is lost and Ig replacement therapy do not substitute for a specific
354 autologous IgG response. We therefore propose that IgA supplementation might have
355 beneficial effects on gut dysbiosis and systemic inflammatory disorders associated with
356 antibody deficiencies. IgA might be orally delivered through a carrier system allowing colon
357 delivery. Polymers such as gellan gum or pectin, are degraded specifically by the colonic
358 microbiota and could thus release polymer-bound IgA locally ³⁶.

359

360 In summary, we report for the first time a systemic anti-commensal IgG response that is
361 restricted to intestinal IgA-coated bacteria in humans. We demonstrate that in the absence of
362 IgA, anti-commensal IgG responses are amplified and associated with reduced systemic
363 inflammation. Finally, the present study provides new therapeutic perspectives based on IgA

364 supplementation in patients with CVID or SIgAd, while SIgAd -derived IgG supplementation
365 might be considered in CVID.

366

367 **Materials and Methods**

368 *Human samples*

369 Fresh stool and blood samples were simultaneously collected from n=30 healthy donors, n=15
370 selective IgA deficiency and n=10 common variable immunodeficiency patients.

371 Healthy donors were recruited among laboratory staff and relatives. Patients followed for
372 clinical manifestations associated with antibody deficiencies were recruited from two French
373 clinical immunology referral centers (Department of Clinical Immunology at Saint Louis
374 hospital and Department of Internal Medecine at Pitié-Salpêtrière hospital, Paris). Patient's
375 inclusion criteria were (i) undetectable seric IgA levels (<0,07 mg/mL) in at least three
376 previous samples in the past year (ii) either selective IgA deficiency (n=15 selective IgA
377 deficient patients), or associated with IgG and/or IgM deficiency integrating a global antibody
378 production defect (n=10 CVID patients). Clinical and biological data were collected at
379 inclusion time.

380 Surgical samples from histologically normal intestine were obtained from twelve donors
381 undergoing gastric bypass or tumorectomy at Pitié-Salpêtrière hospital, Paris.

382

383 Oral and written consent were obtained from patients and healthy donors before inclusion in
384 the study.

385

386 *PBMC and plasma*

387 30 mL of blood were collected in ACD tubes (BD Vacutainer®) and PBMC were isolated by
388 density gradient procedure (Ficoll 400, Eurobio, Les Ulis, France) and then stored in liquid

389 nitrogen after soft freezing in isopropanol. Supernatants were collected as plasma and
390 immediately stored at -80°C.

391

392 ***Stool collection and whole microbiota purification***

393 Stool were collected immediately after emission in a container allowing anaerobic bacteria
394 preservation (Anaerocult band, Merck, Darmstadt, Germany), aliquoted in a CO₂-rich O₂-low
395 atmosphere and stored at -80°C. Fecal microbiota were extracted by gradient purification in
396 anaerobic conditions (Freter chamber) as previously described³⁷. Briefly, thawed feces were
397 diluted in 1x-PBS (Eurobio), 0,03% w/v sodium deoxycholate (NaDC), 60% w/v Nycodenz
398 (Sigma-aldrich, St Louis, USA) and loaded on a continuous density gradient obtained by a
399 freezing-thawing cycle of a Nycodenz solution. Fecal bacteria were obtained after
400 ultracentrifugation (14567 x g, 45 min, +4°C) (Beckman Coulter ultracentrifuge, swinging
401 rotor SW28) and washed three times in 1x-PBS (Eurobio), 0,03% w/v sodium NaDC. The
402 final pellet was diluted in 1xPBS-10%Glycerol, immediately frozen in liquid nitrogen and
403 then stored at -80°C.

404

405 ***Bacterial Flow Cytometry***

406 Specific seric antibodies levels against purified microbiota or cultivable strains were assessed
407 by a flow cytometry assay as previously described¹¹. Briefly, 10⁷ bacteria (purified
408 microbiota or cultivable strains) were fixed in a solution of 4% paraformaldehyde and
409 simultaneously stained with a cell proliferation dye (eFluor 450, eBiosciences, CA, USA).
410 After washing with 1mL of a 1x-PBS solution, cells were resuspended to a final concentration
411 of 4.10⁸ bacteria/mL in a 1x-PBS, 2% w/v BSA, 0.02% w/v Sodium azide solution. Then 10⁷
412 bacteria were incubated in a 96-V bottom well plate with a 10µg/mL IgG solution (from
413 either human serum or pooled human IgG Hizentra[®] - CSL Behring France or human anti-

414 TNF Remicade[®] - MSD France) per condition. Immune complexes were washed twice with a
415 1x-PBS, 2% w/v BSA, 0.02% w/v Sodium azide (200 μ L/well, 4000 x g, 10 minutes, +4°C)
416 and then incubated with secondary conjugated antibodies, either isotype controls mix or goat
417 anti-human IgA-FITC and goat anti-human IgG-A647 (Jackson Immunoresearch
418 Laboratories, West Grove, USA). Acquisition of the cells events was performed on a FACS
419 CANTO II flow cytometer (Becton Dickinson) after washing and analysis was performed
420 with Flow-Jo software (Treestar, Ashland, USA). Medians of fluorescence were used to
421 measure the seric IgG response levels against the cultivable strains. Intestinal IgA binding
422 was quantified by the same assay without incubation with seric immunoglobulins. Results are
423 expressed as median, minimum and maximum percentages throughout the manuscript.

424

425 ***Cytokines quantification***

426 IL-6 and IL-10 were measured in the serum using a 3-step digital assay relying on Single
427 Molecule Array (Simoa) technology HD-1 Analyzer (Quanterix Corporation, Lexington,
428 USA). Working dilutions were 1/4 for all sera in working volumes of 25 μ L. Lower limit of
429 quantification for IL-6 and IL-10 are respectively of 0.01, 0.021 pg/mL.

430

431 ***Soluble CD14 quantification***

432 Soluble CD14 was quantified in plasma (400-fold dilution) by ELISA (Quantikine[®] ELISA
433 kit, R&D, Minneapolis, USA). Experimental procedure followed the manufacturer's
434 recommendations. Lower limit of quantification for soluble CD14 is of 6 pg/mL.

435

436 ***Peripheral blood mononuclear cell phenotyping***

437 T cell phenotyping was performed using a combination of the following antibodies : CD3-
438 H500, CCR7-PE-Cy7, CD4-APC-Cy7 (BD Biosciences), CD45RA-PerCP Cy5.5 (e-

439 Bioscience), CD8-A405 (Invitrogen), CD279-APC (BioLegend). Acquisition of cells events
440 was performed using a FACS CANTO II flow cytometer (Becton Dickinson) and analysis
441 was performed using the Flow-Jo software (Treestar).

442

443 *Intestinal B cells phenotyping*

444 Lamina propria was digested by collagenase A (Roche) in RPMI (Life Technologies) for 30
445 minutes at 37°C. Lymphocytes were purified by centrifugation over Ficoll 400 (Eurobio) and
446 stained with the following antibodies: anti-CD45 APC-H7, anti-CD19 BV421, anti-IgD FITC,
447 anti-CD27 PE-Cy7 (all purchased from BD Biosciences), and anti-IgA PE (Jackson
448 Immunoresearch), or anti-IgG1 PE, anti-IgG2 AF488, anti-IgG3 A647 (Southern Biotech).
449 Dead cells were excluded with LIVE/DEAD™ Fixable Aqua Dead Cell Stain Kit
450 (Invitrogen). Acquisition of cells events was performed using a FACS CANTO II flow
451 cytometer (Becton Dickinson) and analysis was performed using the Flow-Jo software
452 (Treestar).

453

454 *Analysis of IgG-coated bacteria*

455 Purified microbiota (10^9 /condition) was washed in 1x-PBS and stained with isotype control
456 (A647-conjugated Goat IgG, Jackson Immunoresearch Laboratories) as a negative control or
457 anti-human IgG-A647 (Jackson Immunoresearch Laboratories). Acquisition and sorting were
458 performed on a 2 lasers- 2 ways Fluorescent-activated cell sorter (S3 cell sorter, Bio-Rad
459 Laboratories, California, USA). 10^6 bacteria per fraction were collected and immediately
460 stored at -80°C as dry pellets. Purity for both fractions was systematically verified after
461 sorting with a minimum rate of 80%. Genomic DNA was extracted and the V3–V4 region of
462 the 16S rRNA gene was amplified by semi-nested PCR. Primers V3fwd (+357): 5'
463 TACGGRAGGCAGCAG 3' and V4rev (+857): 5' ATCTTACCAGGGTATCTAATCCT 3'

464 were used during the first round of PCR (10 cycles). Primers V3fwd and X926_Rev (+926) 5'
465 CCGTCAATTCMTTTRAGT 3' were used in the second PCR round (40 cycles). Polymerase
466 chain reaction amplicon libraries were sequenced using a MiSeq Illumina platform (Genotoul,
467 Toulouse, France). The open source software package Quantitative Insights Into Microbial
468 Ecology (QIIME) ³⁸ was used to analyse sequences with the following criteria: (i) minimum
469 and maximum read length of 250 bp and 500 bp respectively, (ii) no ambiguous base calls,
470 (iii) no homopolymeric runs longer than 8 bp and (iv) minimum average Phred score > 27
471 within a sliding window of 50 bp. Sequences were aligned with NAST against the
472 GreenGenes reference core alignment set (available in QIIME as
473 core_set_aligned.fasta.imputed) using the 'align_seqs.py' script in QIIME. Sequences that did
474 not cover this region at a percent identity > 75% were removed. Operational taxonomic units
475 were picked at a threshold of 97% similarity using cd-hit from 'pick_otus.py' script in
476 QIIME. Picking workflow in QIIME with the cd-hit clustering method currently involves
477 collapsing identical reads using the longest sequence-first list removal algorithm, picking
478 OTU and subsequently inflating the identical reads to recapture abundance information about
479 the initial sequences. Singletons were removed, as only OTU that were present at the level of
480 at least two reads in more than one sample were retained (9413 ± 5253 sequences per
481 sample). The most abundant member of each OTU was selected through the 'pick_rep_set.py'
482 script as the representative sequence. The resulting OTU representative sequences were
483 assigned to different taxonomic levels (from phylum to genus) using the GreenGenes database
484 (release August 2012), with consensus annotation from the Ribosomal Database Project naïve
485 Bayesian classifier [RDP 10 database, version 6 ³⁹. To confirm the annotation, OTU
486 representative sequences were then searched against the RDP database, using the online
487 program seqmatch (http://rdp.cme.msu.edu/seqmatch/seqmatch_intro.jsp) and a threshold
488 setting of 90% to assign a genus to each sequence.

489

490 ***Immunoblotting***

491 10⁸ CFU of wild type *Escherichia coli* were freezed (-80°C) and thawed (37°C) three times in
492 30µL of lysis buffer (50mM Tris-HCL, 8M urea). Lysis efficiency was verified by Gram
493 staining. Proteins were separated using 4%-20% polyacrylamide gel electrophoresis (Mini-
494 PROTEAN TGX Stain-Free Precast Gels; Bio-Rad) in reducing conditions (dithiothreitol
495 DTT and sodium dodecyl sulfate SDS, Bio-Rad) and transferred to nitrocellulose. Membranes
496 were incubated with 10µg/ml of human seric IgG or IgA of different healthy donors. Human
497 IgG were detected with horseradish peroxidase-conjugated goat anti-human IgG used at
498 1:50,000 or goat anti-human IgG used at 1:20,000 followed by enhanced chemi-luminescence
499 revealing reaction (Clarity™ Western ECL, Bio-Rad). Human IgA were detected with
500 horseradish peroxidase-conjugated goat anti-human IgA used at 1:20 000 (Bethyl
501 Laboratories). All incubations were in 1x-PBS with 5% non fat milk and washing steps in 1x-
502 PBS with 0.1% Tween.

503

504 ***IgG gene expression analysis***

505 Total RNA of jejunal lamina propria fraction and PBMC were extracted with the RNeasy
506 Mini kit (QIAGEN). cDNAs were synthesized from and prepared with M-MLV reverse
507 transcriptase (Promega). SYBR green primers were designed by manufacturer (Roche) and
508 used for qRT-PCR using the 7300 real time PCR system (Applied Biosystem). Data were
509 normalized to ribosomal 18S RNA.

510

511

512

513 **Figure legends:**

514

515 **Figure 1: Systemic IgG and secretory IgA recognize a common spectrum of commensals.**

516 A. Representative flow cytometry dot plot showing from bottom to top isotype control,
517 endogenous secretory IgA (without serum), human IgG anti-TNF (10 μ g/ml ; irrelevant
518 IgG) and autologous systemic IgG (10 μ g/ml) to fecal microbiota in a healthy donor.

519 B. Flow cytometry analysis of the fraction of fecal microbiota bound by either secretory
520 IgA, seric IgG or both in healthy donors (n=30). Median values are indicated and
521 subgroups are compared with a non-parametric Mann-Whitney test.

522

523 **Figure 2 : Systemic IgG bind a broad spectrum of commensals**

524 A. Flow cytometry analysis of serum IgG binding to cultivated bacterial strains. Grey
525 histograms represent isotype controls and dark lines anti-IgG staining.

526 B. Flow cytometry analysis of serum IgG binding levels to 8 different bacterial strains in
527 healthy donors (n=30). Blue strains (left) are typically poorly coated by secretory IgA
528 from healthy individuals while pink strains (right) are representative of typical IgA
529 targets¹⁵. Results are presented as Δ Median Fluorescence Intensity (MFI) *i.e.*: IgG =
530 MFI IgG serum – MFI IgG negative control. Red bars show medians. Kruskal-wallis
531 test was used to calculate p-value.

532 C. Representative immunoblotting of *Escherichia coli* lysates probed with five different
533 healthy human serums, with a normalized IgA and IgG levels. Ponceau staining
534 indicates total amounts of bacteria lysates loaded. IgA and IgG binding were assessed
535 by an HRP conjugated secondary antibody.

536

537 **Figure 3: IgA deficient patients harbour private anti-commensal IgG responses.**

- 538 A. Flow cytometry analysis of fecal microbiota bound by autologous seric IgG in healthy
539 donors (n=30) and IgA deficient patients (n=15). Red bars represent medians. P-value
540 was calculated by Mann-Whitney test.
- 541 B. Representative flow cytometry analysis of autologous seric IgG binding (left) or
542 polyclonal IgG derived from pooled serum of healthy donors binding (right) to fecal
543 microbiota. In a healthy donor (top) and in an IgA deficient patient (bottom).
- 544 C. Flow cytometry analysis of the IgG-bound fecal microbiota with IgG from autologous
545 serum or polyvalent IgG in healthy donors (n=30) and IgA deficient patients (n=15).
546 P-values were calculated by Wilcoxon-paired test.
- 547 D. Flow cytometry detection of IgG on IgA deficient microbiota (n=9), following
548 incubation with autologous serum or heterologous serum from another, randomly
549 picked, IgA deficient individual. P-value was calculated by Wilcoxon-paired test.

550

551 **Figure 4: Private IgG anti-microbial signatures.**

- 552 A. Sorting strategy of IgG-bound and IgG-unbound microbiota in 10 healthy donors and
553 3 IgA deficient patients. Composition of sorted subsets was next analysed by 16S
554 rRNA sequencing.
- 555 B. Genera diversity in IgG+ and IgG- sorted fractions calculated by Shannon index. Dark
556 symbols correspond to healthy donors, red symbols to IgA deficient patients.
- 557 C. Median relative abundance of genera in IgG+ and IgG- sorted fractions. Dark symbols
558 correspond to healthy donors, red symbols to IgA deficient patients.
- 559 D. IgG responses toward the 30 most frequent genera in 10 healthy donors. IgG response
560 to a given bacteria is expressed as a calculated IgG index (as defined in the box),
561 outlining genera more likely serum IgG-bound in red.- Genera and individuals are
562 grouped using a hierarchical clustering algorithm.

563 E. IgG responses (defined by IgG index) toward the 30 most frequent genera in 3 IgA
564 deficient patients.

565

566 **Figure 5: Microbiota specific IgG and inflammation**

567 A. Percentage of serum IgG-bound microbiota correlated with sCD14 levels in
568 autologous serum of healthy donors (triangles) and SIgAd patients (dark points).
569 Spearman coefficient (r) and p-value (p) are indicated.

570 B. Flow cytometry analysis of IgG-bound microbiota following IVIG exposure in healthy
571 donors and CVID patients.

572 C. sCD14 levels measured by ELISA in plasmas of healthy donors and CVID patients.

573 D. Seric IL-6 levels measured by Simoa technology in plasmas of healthy donors and
574 CVID patients.

575 E. Flow cytometry analysis of CD4+CD45RA-PD-1+ lymphocytes in peripheral blood
576 mononuclear cells of healthy donors and CVID patients. Percentage among CD4+ T
577 cells is presented.

578 For all dot plots, black lines represent medians. Mann-Whitney test was used to calculate p-
579 values (*p<0.05, ***p<0.001)

580

581 **Figure S1: *In vivo* intestinal IgG binding to gut microbiota**

582 Flow cytometry analysis of the fraction of fecal microbiota bound by intestinal IgG in healthy
583 donors (HD; n=30) and selective IgA deficient patients (SIgAd; n=15). Pink bars represent
584 medians.

585

586 **Figure S2: Anti-commensals IgG react mostly in a Fab-dependent manner**

587 (A-B) Flow cytometry analysis of 30 healthy (A) and 15 IgA deficient (B) fecal microbiota

588 samples incubated with seric IgG or human IgG anti-TNF $\text{TNF}\alpha$.

589 (C) Flow cytometry analysis of 10 IgA deficient fecal microbiota samples incubated with
590 heterologous seric IgG or human IgG anti-TNF $\text{TNF}\alpha$.

591 Wilcoxon-paired test was used to calculate p-values. **p<0.01;***p<0.001; ****p<0.0001

592

593 **Figure S3: Anti-commensals IgG are mostly of IgG2 isotype**

594 A. Representative flow cytometry analysis of serum IgG1, IgG2, IgG3 and IgG4 binding
595 to *Bifidobacterium adolescentis*. Grey histograms represent serum from an IgG2
596 deficient patient that served as negative control, red histograms represent serum from
597 a healthy donor. This donor was scored IgG2+ and IgG1- against *Bifidobacterium*
598 *adolescentis*.

599 B. Flow cytometry analysis of IgG1, IgG2, IgG3 and IgG4 binding to *Bifidobacterium*
600 *adolescentis*, *Bifidobacterium longum* and *Escherichia coli* in 30 healthy donors.

601

602 **Figure S4: IgG2+ B cells are present in human gut lamina propria.**

603 A. Proportions of surface IgA+, IgG1+, IgG2+, or IgG3+ cells among lamina propria
604 CD19+CD27+IgD- switched B cells were detected by flow cytometry in jejunum (n =
605 4, pink symbols), ileum (n = 2, black symbols) or colon (n = 2, blue symbols) samples.

606 B. Cgamma transcripts were determined by RT-qPCR in lamina propria (LP) and
607 peripheral blood mononuclear cells (PBMC) from 4 severely obese patients. Results
608 are expressed as fold expression in LP over PBMC (mean \pm SEM)

609

610

611

612 **References**

613

- 614 1. Honda K, Littman DR. The microbiota in adaptive immune homeostasis and disease.
615 Nature. 2016;535:75.
- 616 2. Slack E, Hapfelmeier S, Stecher B, Velykoredko Y, Stoel M, Lawson MAE, et al.
617 Innate and adaptive immunity cooperate flexibly to maintain host-microbiota mutualism.
618 Science. 2009;325:617–20.
- 619 3. Donskey CJ. The role of the intestinal tract as a reservoir and source for transmission
620 of nosocomial pathogens. Clin Infect Dis Off Publ Infect Dis Soc Am. 2004;39:219–26.
- 621 4. MacFie J. Current status of bacterial translocation as a cause of surgical sepsis. Br
622 Med Bull. 2004;71:1–11.
- 623 5. Beaugerie L, Sokol H. Clinical, serological and genetic predictors of inflammatory
624 bowel disease course. World J Gastroenterol. 2012;18:3806–13.
- 625 6. Johansen FE, Pekna M, Norderhaug IN, Haneberg B, Hietala MA, Krajci P, et al.
626 Absence of epithelial immunoglobulin A transport, with increased mucosal leakiness, in
627 polymeric immunoglobulin receptor/secretory component-deficient mice. J Exp Med.
628 1999;190:915–22.
- 629 7. Koch MA, Reiner GL, Lugo KA, Kreuk LSM, Stanbery AG, Ansaldo E, et al.
630 Maternal IgG and IgA Antibodies Dampen Mucosal T Helper Cell Responses in Early Life.
631 Cell. 2016;165:827–41.
- 632 8. Zeng MY, Cisalpino D, Varadarajan S, Hellman J, Warren HS, Cascalho M, et al. Gut
633 Microbiota-Induced Immunoglobulin G Controls Systemic Infection by Symbiotic Bacteria
634 and Pathogens. Immunity. 2016;44:647–58.
- 635 9. Benckert J, Schmolka N, Kreschel C, Zoller MJ, Sturm A, Wiedenmann B, et al. The
636 majority of intestinal IgA+ and IgG+ plasmablasts in the human gut are antigen-specific. J

- 637 Clin Invest. 2011;121:1946–55.
- 638 10. Iversen R, Snir O, Stensland M, Kroll JE, Steinsbø Ø, Korponay-Szabó IR, et al.
639 Strong Clonal Relatedness between Serum and Gut IgA despite Different Plasma Cell
640 Origins. *Cell Rep.* 2017;20:2357–67.
- 641 11. Moor K, Fadlallah J, Toska A, Sterlin D, Balmer ML, Macpherson AJ, et al. Analysis
642 of bacterial-surface-specific antibodies in body fluids using bacterial flow cytometry. *Nat*
643 *Protoc.* 2016;11:1531–53.
- 644 12. Palm NW, de Zoete MR, Cullen TW, Barry NA, Stefanowski J, Hao L, et al.
645 Immunoglobulin A coating identifies colitogenic bacteria in inflammatory bowel disease.
646 *Cell.* 2014;158:1000–10.
- 647 13. D’Auria G, Peris-Bondia F, Džunková M, Mira A, Collado MC, Latorre A, et al.
648 Active and secreted IgA-coated bacterial fractions from the human gut reveal an under-
649 represented microbiota core. *Sci Rep.* 2013;3:3515.
- 650 14. Kau AL, Planer JD, Liu J, Rao S, Yatsunenکو T, Trehan I, et al. Functional
651 characterization of IgA-targeted bacterial taxa from undernourished Malawian children that
652 produce diet-dependent enteropathy. *Sci Transl Med.* 2015;7:276ra24.
- 653 15. Fadlallah J, El Kafsi H, Sterlin D, Juste C, Parizot C, Dorgham K, et al. Microbial
654 ecology perturbation in human IgA deficiency. *Sci Transl Med.* 2018;10.
- 655 16. Sokol H, Pigneur B, Watterlot L, Lakhdari O, Bermúdez-Humarán LG, Gratadoux J-J,
656 et al. *Faecalibacterium prausnitzii* is an anti-inflammatory commensal bacterium identified by
657 gut microbiota analysis of Crohn disease patients. *Proc Natl Acad Sci U S A.*
658 2008;105:16731–6.
- 659 17. Bazil V, Strominger JL. Shedding as a mechanism of down-modulation of CD14 on
660 stimulated human monocytes. *J Immunol Baltim Md 1950.* 1991;147:1567–74.
- 661 18. Perreau M, Vigano S, Bellanger F, Pellaton C, Buss G, Comte D, et al. Exhaustion of

662 bacteria-specific CD4 T cells and microbial translocation in common variable
663 immunodeficiency disorders. *J Exp Med*. 2014;211:2033–45.

664 19. Landers CJ, Cohavy O, Misra R, Yang H, Lin Y-C, Braun J, et al. Selected loss of
665 tolerance evidenced by Crohn's disease-associated immune responses to auto- and microbial
666 antigens. *Gastroenterology*. 2002;123:689–99.

667 20. Macpherson A, Khoo UY, Forgacs I, Philpott-Howard J, Bjarnason I. Mucosal
668 antibodies in inflammatory bowel disease are directed against intestinal bacteria. *Gut*.
669 1996;38:365–75.

670 21. Wilmore JR, Gaudette BT, Gomez Atria D, Hashemi T, Jones DD, Gardner CA, et al.
671 Commensal Microbes Induce Serum IgA Responses that Protect against Polymicrobial
672 Sepsis. *Cell Host Microbe*. 2018;23:302–311.e3.

673 22. Russell MW, Mansa B. Complement-fixing properties of human IgA antibodies.
674 Alternative pathway complement activation by plastic-bound, but not specific antigen-bound,
675 IgA. *Scand J Immunol*. 1989;30:175–83.

676 23. Bindon CI, Hale G, Brüggemann M, Waldmann H. Human monoclonal IgG isotypes
677 differ in complement activating function at the level of C4 as well as C1q. *J Exp Med*.
678 1988;168:127–42.

679 24. Bruhns P, Iannascoli B, England P, Mancardi DA, Fernandez N, Jorieux S, et al.
680 Specificity and affinity of human Fcγ receptors and their polymorphic variants for
681 human IgG subclasses. *Blood*. 2009;113:3716–25.

682 25. Nimmerjahn F, Gordan S, Lux A. FcγR dependent mechanisms of cytotoxic,
683 agonistic, and neutralizing antibody activities. *Trends Immunol*. 2015;36:325–36.

684 26. White AL, Chan HTC, French RR, Willoughby J, Mockridge CI, Roghanian A, et al.
685 Conformation of the human immunoglobulin G2 hinge imparts superagonistic properties to
686 immunostimulatory anticancer antibodies. *Cancer Cell*. 2015;27:138–48.

- 687 27. Schneider C, Smith DF, Cummings RD, Boligan KF, Hamilton RG, Bochner BS, et
688 al. The human IgG anti-carbohydrate repertoire exhibits a universal architecture and contains
689 specificity for microbial attachment sites. *Sci Transl Med.* 2015;7:269ra1.
- 690 28. Bunker JJ, Erickson SA, Flynn TM, Henry C, Koval JC, Meisel M, et al. Natural
691 polyreactive IgA antibodies coat the intestinal microbiota. *Science.* 2017;
- 692 29. Christmann BS, Abrahamsson TR, Bernstein CN, Duck LW, Mannon PJ, Berg G, et
693 al. Human seroreactivity to gut microbiota antigens. *J Allergy Clin Immunol.* 2015;136:1378-
694 1386-5.
- 695 30. Bunker JJ, Flynn TM, Koval JC, Shaw DG, Meisel M, McDonald BD, et al. Innate
696 and Adaptive Humoral Responses Coat Distinct Commensal Bacteria with Immunoglobulin
697 A. *Immunity.* 2015;43:541–53.
- 698 31. Okai S, Usui F, Yokota S, Hori-i Y, Hasegawa M, Nakamura T, et al. High-affinity
699 monoclonal IgA regulates gut microbiota and prevents colitis in mice. *Nat Microbiol.*
700 2016;1:16103.
- 701 32. Rollenske T, Szijarto V, Lukasiewicz J, Guachalla LM, Stojkovic K, Hartl K, et al.
702 Cross-specificity of protective human antibodies against *Klebsiella pneumoniae* LPS O-
703 antigen. *Nat Immunol.* 2018;19:617–24.
- 704 33. Jørgensen SF, Trøseid M, Kummen M, Anmarkrud JA, Michelsen AE, Osnes LT, et
705 al. Altered gut microbiota profile in common variable immunodeficiency associates with
706 levels of lipopolysaccharide and markers of systemic immune activation. *Mucosal Immunol.*
707 2016;9:1455–65.
- 708 34. Favre O, Leimgruber A, Nicole A, Spertini F. Intravenous immunoglobulin
709 replacement prevents severe and lower respiratory tract infections, but not upper respiratory
710 tract and non-respiratory infections in common variable immune deficiency. *Allergy.*
711 2005;60:385–90.

- 712 35. Gomez de Agüero M, Ganal-Vonarburg SC, Fuhrer T, Rupp S, Uchimura Y, Li H, et
713 al. The maternal microbiota drives early postnatal innate immune development. *Science*.
714 2016;351:1296–302.
- 715 36. Sandolo C, Péchiné S, Le Monnier A, Hoys S, Janoir C, Coviello T, et al.
716 Encapsulation of Cwp84 into pectin beads for oral vaccination against *Clostridium difficile*.
717 *Eur J Pharm Biopharm Off J Arbeitsgemeinschaft Pharm Verfahrenstechnik EV*.
718 2011;79:566–73.
- 719 37. Juste C, Kreil DP, Beauvallet C, Guillot A, Vaca S, Carapito C, et al. Bacterial protein
720 signals are associated with Crohn’s disease. *Gut*. 2014;63:1566–77.
- 721 38. Caporaso JG, Kuczynski J, Stombaugh J, Bittinger K, Bushman FD, Costello EK, et
722 al. QIIME allows analysis of high-throughput community sequencing data. *Nat Methods*.
723 2010;7:335–6.
- 724 39. Cole JR, Wang Q, Cardenas E, Fish J, Chai B, Farris RJ, et al. The Ribosomal
725 Database Project: improved alignments and new tools for rRNA analysis. *Nucleic Acids Res*.
726 2009;37:D141-145.
- 727

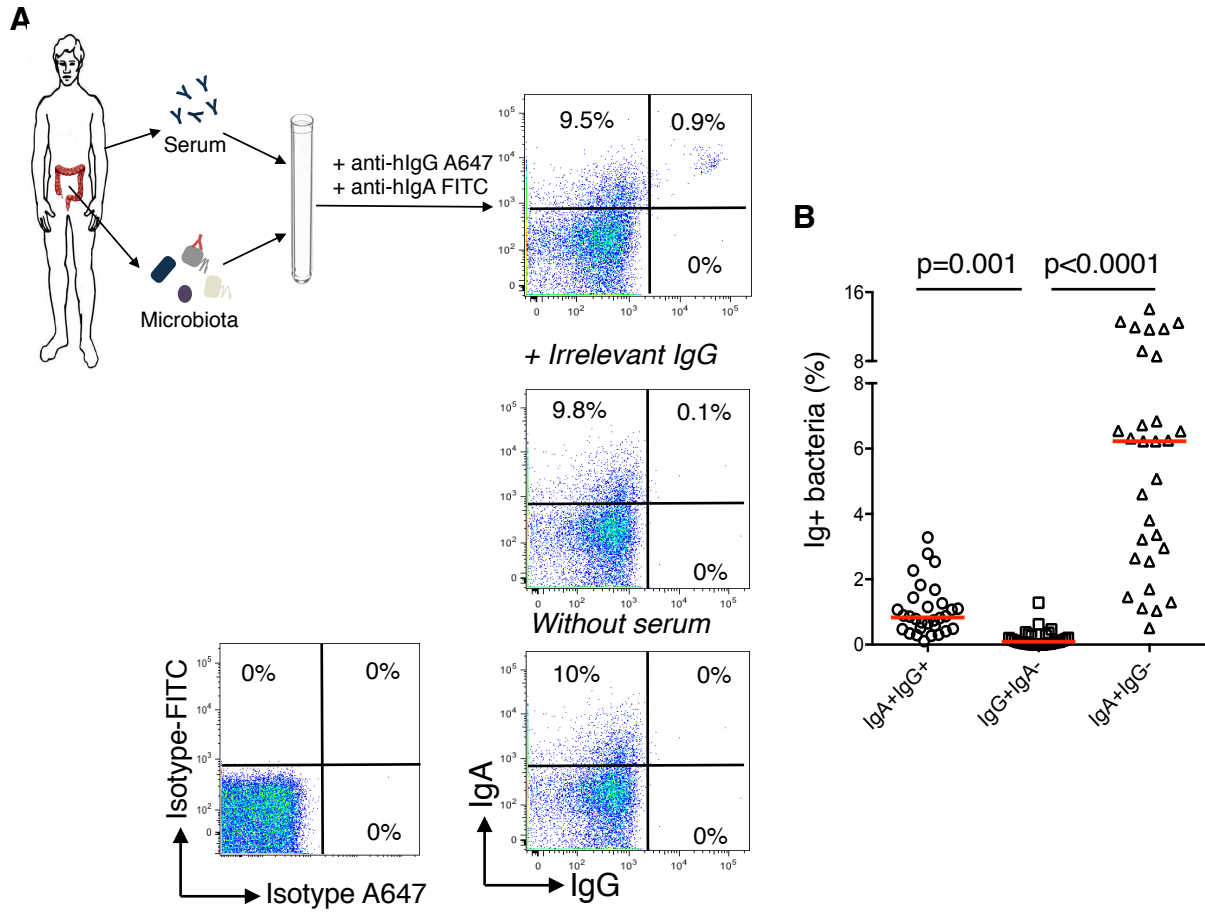


Figure 1

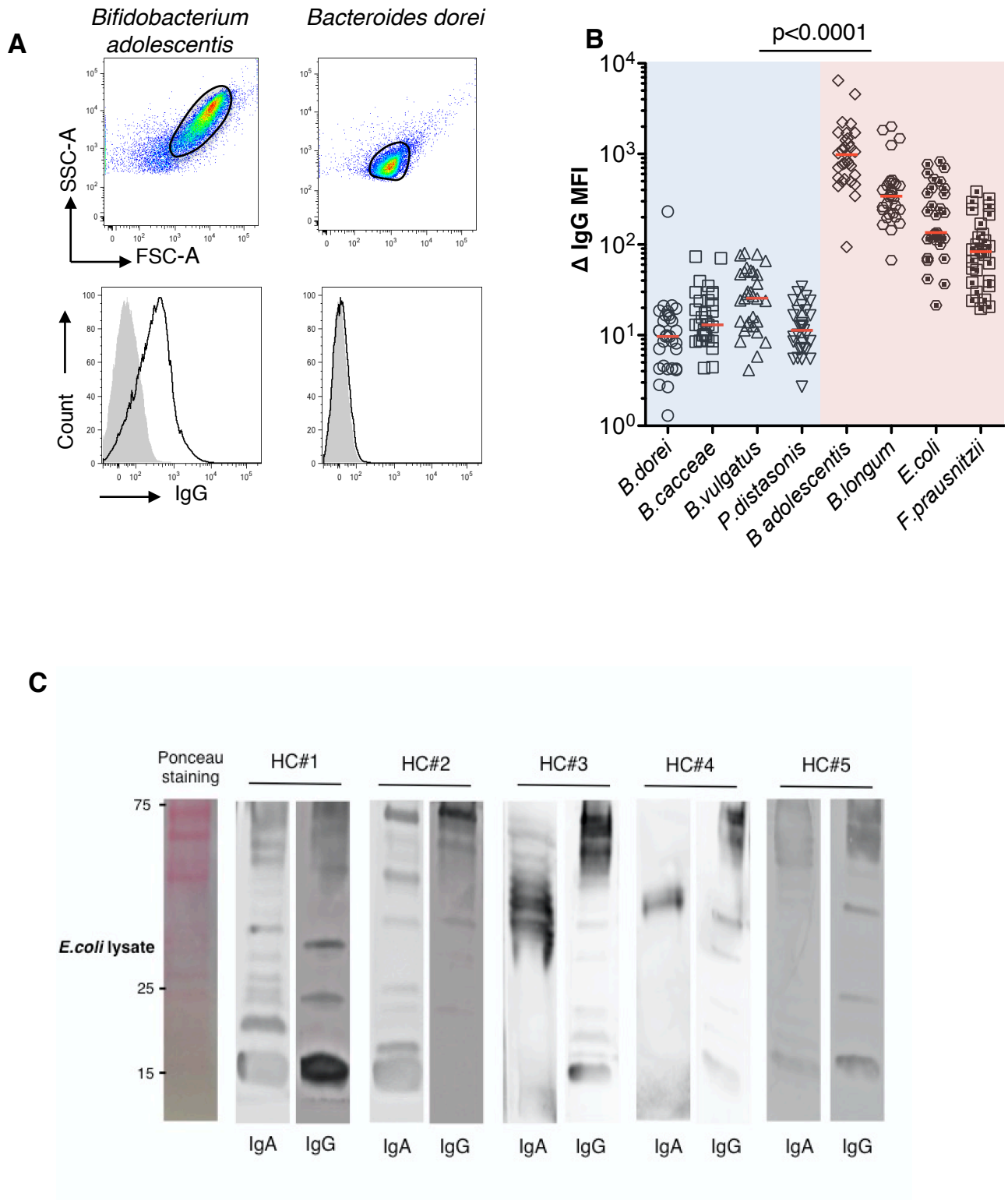


Figure 2

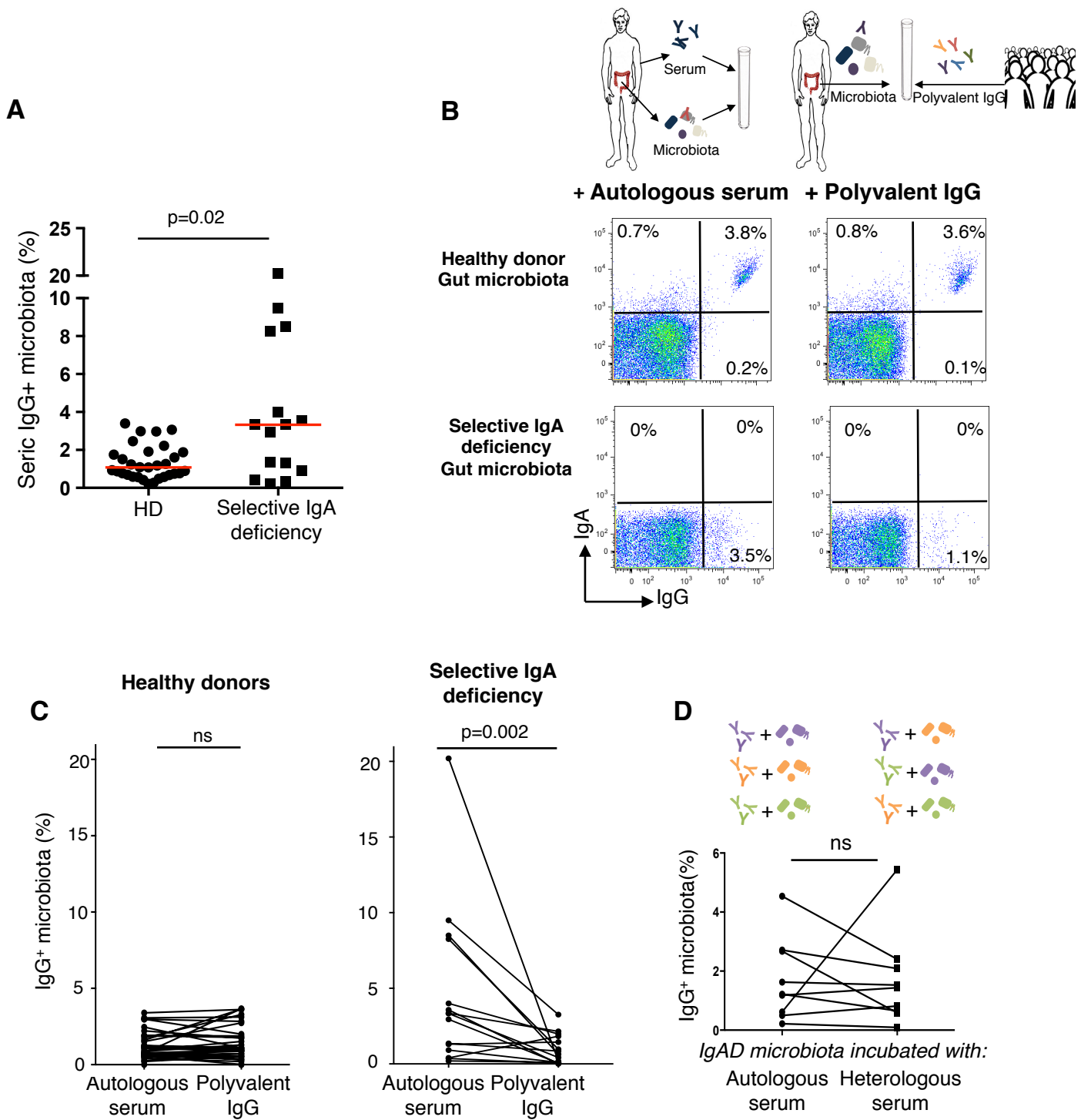


Figure 3

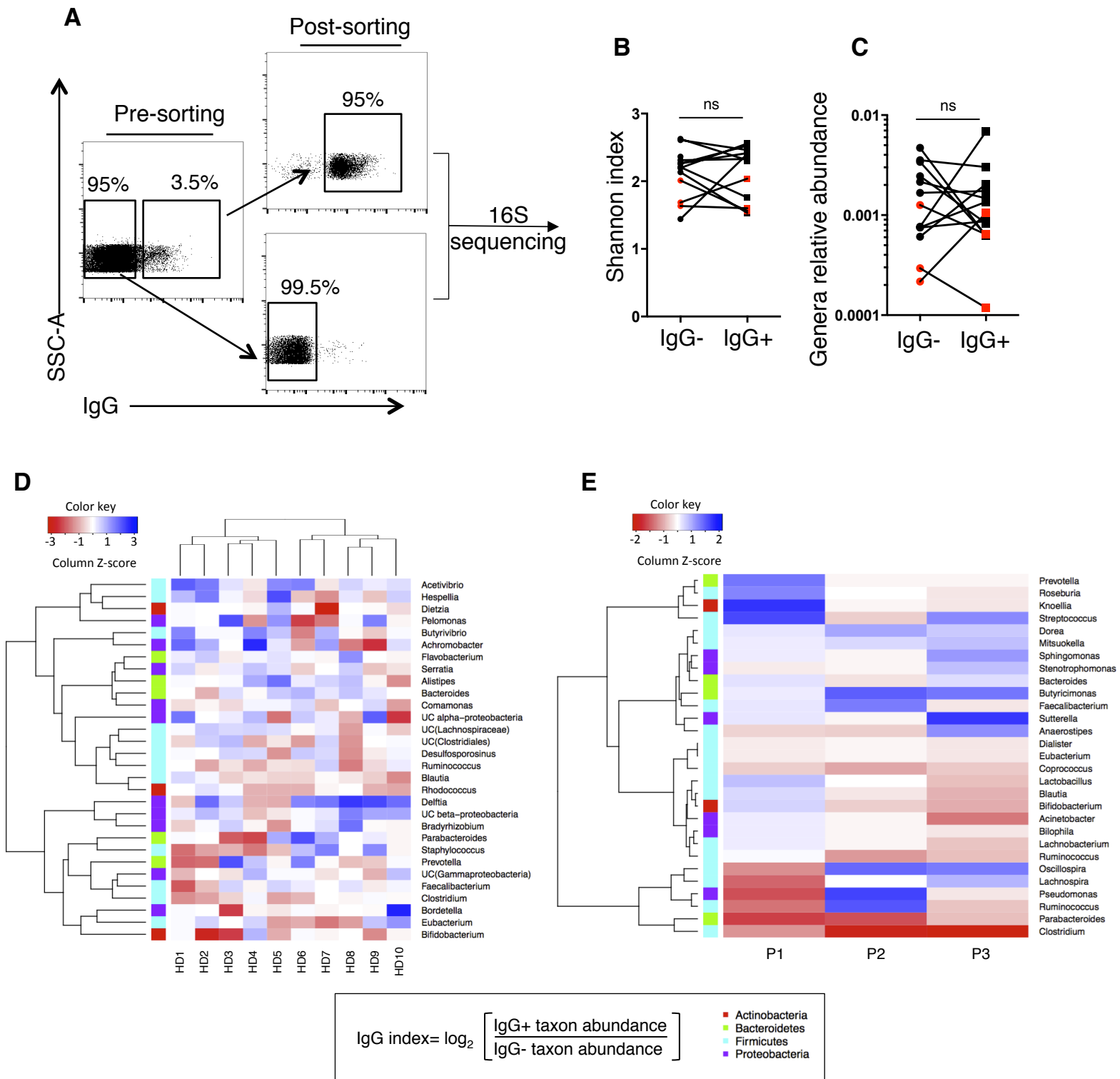


Figure 4

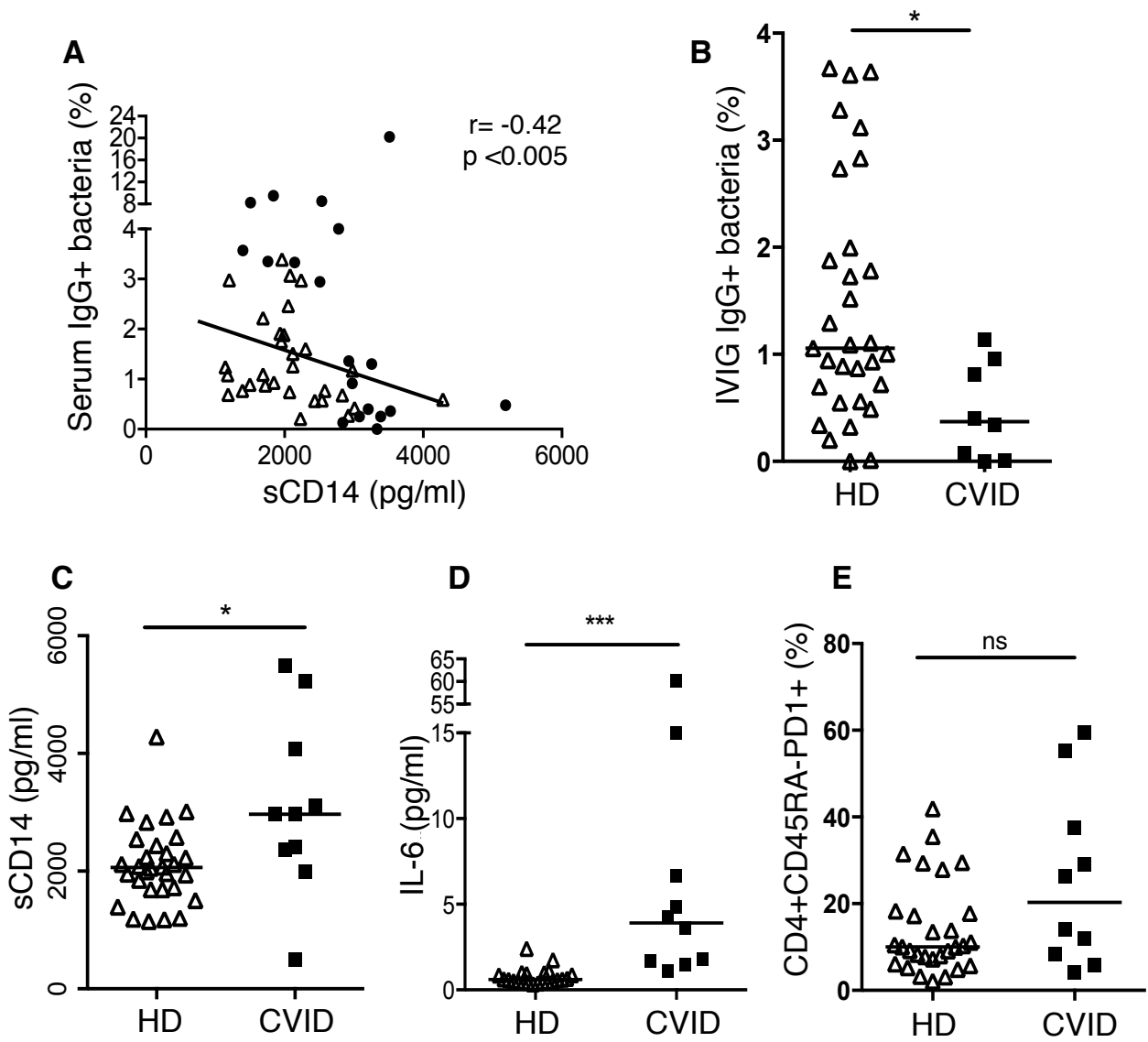


Figure 5

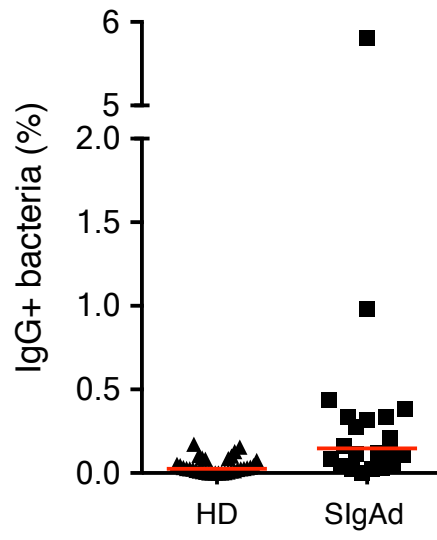


Figure S1

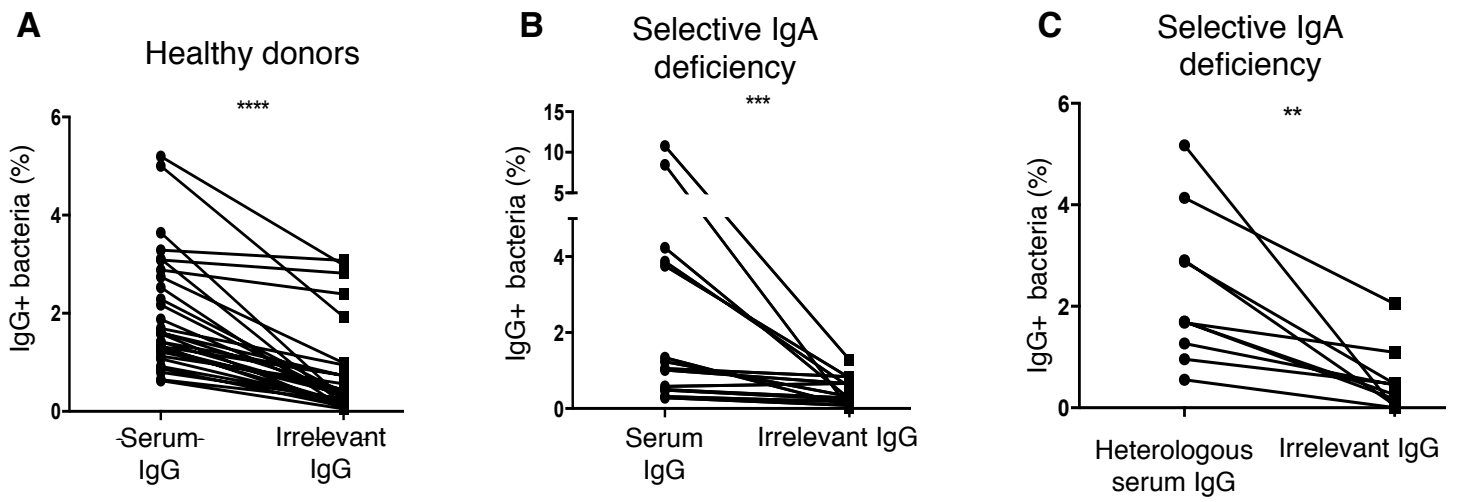


Figure S2

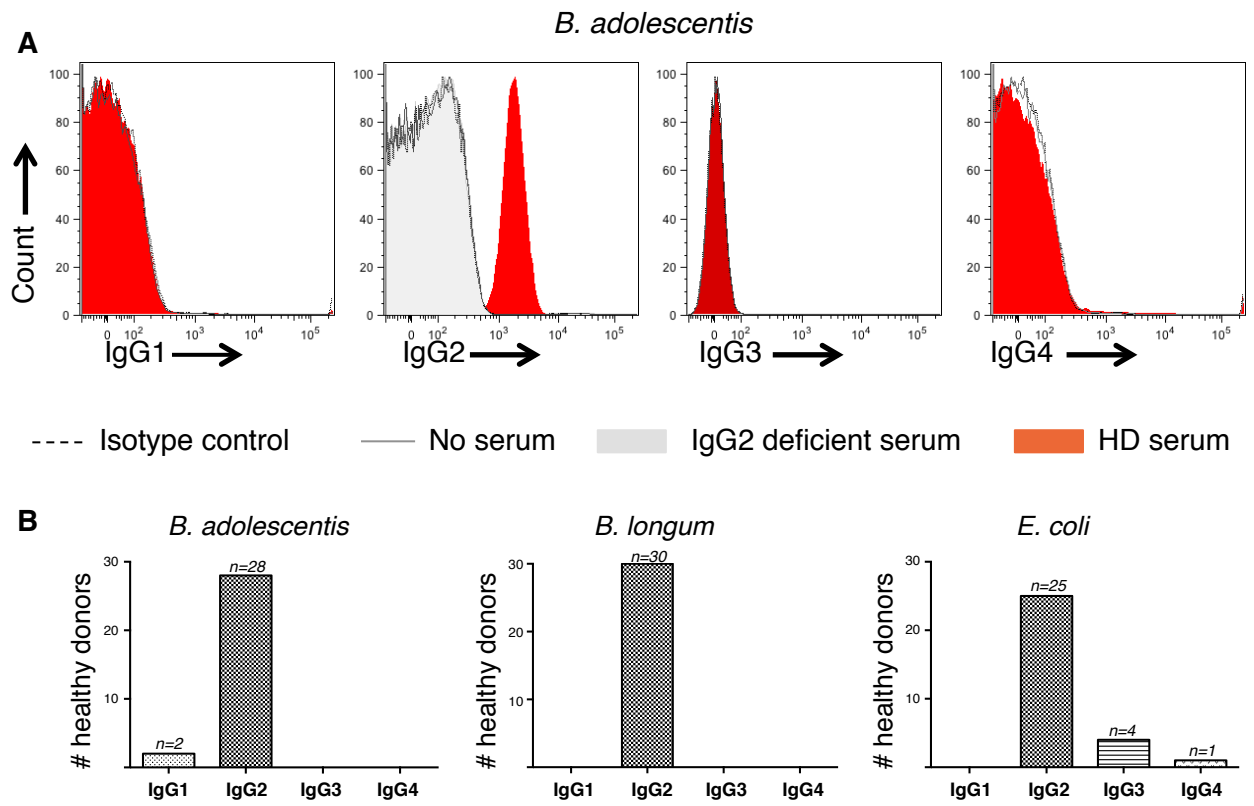


Figure S3

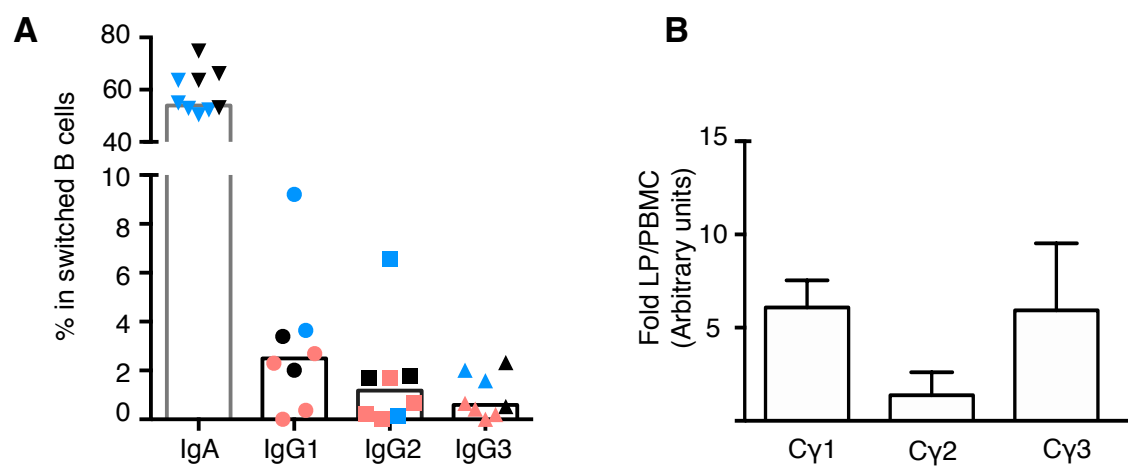


Figure S4